Sky/Ground Segmentation Using Different Approaches

Arlete Teresinha Beuren
Department of Computer Science
Federal University of Technology
Santa Helena (PR), Brazil
arletebeuren@utfpr.edu.br

Alceu de Souza Britto Jr.
Department of Computer Science
Pontifical Catholic University of Paraná
Curitiba (PR), Brazil
alceu@ppgia.pucpr.br

Jacques Facon
Department of Computer Science
Federal University
São Mateus (ES), Brazil
jacques.facon@ufes.br

***Abstract* - This work presents a sky and ground segmentation approach in digital images using the supervised Support Vector Machine (SVM) algorithm based on Whiteness and Blueness indexes, Local Binary Patterns, and Extended morphological profile features. The goal is to separate the image contents in two classes, the sky and the ground. The research is divided into two stages: first, the best features selected by monolithic classifiers using the cross-validation technique. The second stage based on combination of classifiers to segment sky and ground: in a first approach, the strategy consists in segmentation process without dividing the image databases into categories. The second approach carries out segmentation a pre-classification of databases into four categories, City, Highway/Road, Sea/ Harbor, and Nature/Mountain. We used two bases of 1200 images each, containing images with different sky and ground contexts. The first approach is generally adopted in the literature. The second approach, little cited in the literature, presents promising and distinct results for both image bases and allows us to see importance of dividing the images into categories, since there is alteration of the ground context, which leads to different results and greater hit rate.**

Keywords –Shy, Ground, Color index, Segmentation, Classifier.

I. INTRODUCTION

The ability of humans to distinguish the sky from the ground under different circumstances is very large. However, the wide variations of light, brightness and regions make difficult to segment the sky and the ground. We propose the use of the SVM supervised classifier to numerically evaluate the efficiency of different color indexes as whiteness and blueness, LBP features and extended morphological profiles in the sky/ground segmentation task. Figure 1 exemplifies an image with the skyline highlighted.

Fig. 1. Example of an image with the horizon highlighted.

The authors in [1] explain that the horizon line or simply the horizon represents valuable information in aerial images. In the case of digital images and videos, the skyline is used for different purposes, such as guiding sea and air navigation to fly marine vehicles, adjusting flight plans, and make easier surveillance to prevent accidents, particularly collisions with obstacles.

According to [2], many studies assume that the horizon in the image is a straight line with clear edge features, but this assumption is not true under different meteorological and environmental conditions. For example, cloudy sky produces a *weaker* contrast and brightness. Then the horizon edge features, for example, are difficult to define.

Since the sky can also present varied brightness and climate, the soil can be composed of sea, ice, mountains, forests, cities, and thus present different of color and texture patterns, the definition of an automatic approach to segment the sky and the ground in digital images is a more difficult task.

In the study of [3] present a sky/ground segmentation for images of two different glaciers in Alaska. Robust line segments are extracted from the image using the canny edge detector. To compare the results, 100 pictures were selected and manually labeled, indicating the areas of the foreground and background. From the viewpoint of classification, the average error rate was less than 2.5% of the amount of image pixels.

The authors in [4] present an approach to avoid obstacles based on camera image segmentation in sky and not sky regions. The authors used a machine learning process from different types of visual features extracted from the images as a pixel value in the RGB, HSV and YCbCr color spaces.

The work presented in [5] presents a method of sky/earth detection in maritime images using the Hough transform. The images are first filtered by morphological erosion to reduce the probability of weak edge detection in the later stages. They conclude that the angular deviation is very small, being 0.06 degrees on average for infrared images and 0.21 degrees to visible light images.

The authors in [6] propose convolutional neural networks (CNN) trained to detect sky and non-sky regions, as well as the horizon in video frames. The proposed method uses CNN to perform sky detection by generating a binary image where white pixels are classified as sky and black pixels as ground. A base of 13,687 images was built based on video frames specifically for this purpose. The authors state that convolutional neural networks surpass the existing classifiers in the literature.

The approach proposed by [7] presents the sky classification based on whiteness indexes. The features computed through eleven whiteness indexes, still little known and almost exclusively used in the industry, were used to classify the sky and the ground through the SVM supervised

978-1-7281-6926-2/20/$31.00 ©2020 IEEE

classifier. The image bank used in the experiments, with blue, rainy, clear, sunny or cloudy sky, totaled 1200 images and was divided into four categories of 300 images: city, sea, natural landscape and highway images. The authors define some whiteness indexes as promising in the sky/ground segmentation challenge. The average hit rate for the four categories reaches 91, 94%.

II. Present Work

The work is divided into several modules: A) Dataset containing different types of sky and ground, B) Extraction of different features, C) Evaluation of the features using the SVM classifier; and D) Results and Discussion.

A. Database

We built two bases containing 1,200 images each, a base with a wide range of sky (cloudy, rainy, varied light) and another with different terrestrial contexts, without much variation in the sky. Figure 2 depicts some images of the first database called Variation Base mentioned in the experiments in [23]. The second image base called Web Base was built by randomly selecting images on the Web, taking into account different soil contexts, as depicted in Figure 3. Both bases were divided into four categories, City, Highway/Road, Sea/Harbor, and Nature/Mountain and include the respective groundtruth images.

Fig. 2. Examples of images from the Variation Base.

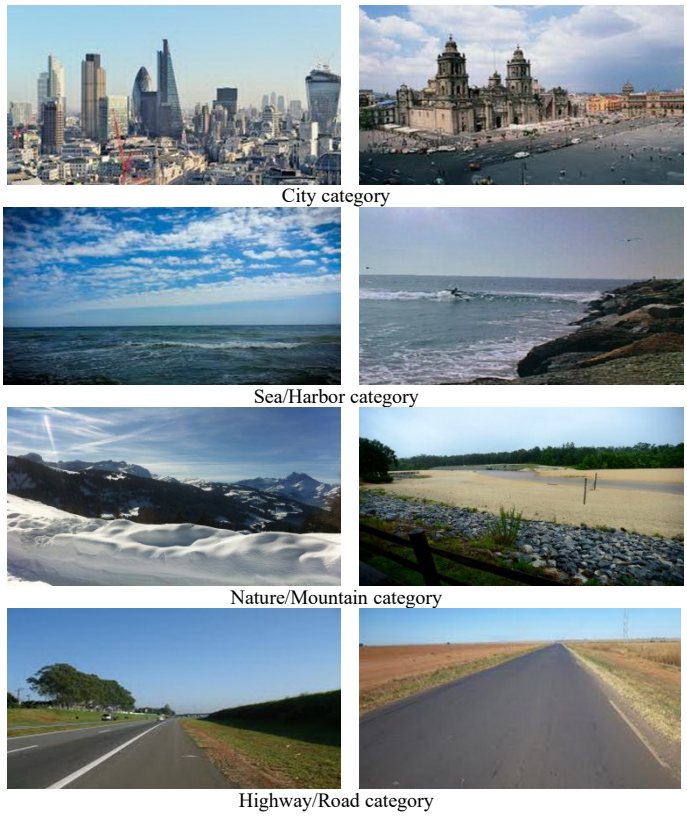

Fig. 3. Examples of images from the Web Base for the City category.

B. Features

The features used in the sky/ground separation task are computed from whiteness and blueness indexes, LBP texture and extended morphological profiles.

- *Whiteness indexes:* Whiteness is an index that measures the relative degree of white. Whiteness indexes are applied in some very specific areas such as dentistry [8] and [7], industrial applications as whitening of materials such as plastic [9]. There are few applications using Whiteness indexes to segment images in the literature.

Next, the whiteness indexes published in the literature and their formulations are listed. Equations with R, G, B in their composition use RGB color space channels. Likewise, equations with H, S, I or H, S, L use the HSI or HSL color spaces, respectively.

a) W_A [9] , [10] $\quad WI = 3.388 * Z - 3 * Y$ (1)

b) W_B [10] , [7] $\quad W_B = Y + a * Z - b * X$ (2)

Where the RGB channels are previously converted to XYZ space. And a and b are observer coefficients:

	a	*b*
2º observer	3.440	3.895
10º observer	3.448	3.904

c) W_S [9] $$W_S = 2B - R \quad (3)$$

d) W_T [9] $$W_T = 4B - 3G \quad (4)$$

e) W_{HL} [9] , [11] $$W_{HL} = L - 3b \quad (5)$$

Where the RGB channels are previously converted to XYZ space. And the conversion of XYZ space to Lab one is defined as follows:

$$L = 100\sqrt{\frac{Y}{Y_n}} \; ; \; a = 175\sqrt{\frac{0.0102 * X_n}{Y / Y_n}} * (\frac{X}{X_n} - \frac{Y}{Y_n})$$

$$b = 70\sqrt{\frac{0.00847 * Z_n}{Y / Y_n}} * (\frac{X}{X_n} - \frac{Z}{Z_n})$$

For luminance D65/10º, Xn, Yn, Zn values are tabulated as follows:

$$Xn = 0.95047; \quad Yn = 1.00000; \quad Zn = 1.08883$$

Each whiteness index is calculated in a 3x3 sliding window on each pixel for the two base images. The result whiteness images were converted to grayscale ones [0-255].

- *Blueness indexes:* The concept of blue is an index that measures the relative degree of blue. These indexes used in applications that measure the amount of blue found in the seas and oceans [12]. Similarly, the image of each blue index is generated by calculating the index in a 3x3 sliding window for the two bases, as described below and then converted to grayscale one [0-255].

a) B_{SI} [13] $$B_{SI} = \frac{DN_B - DN_R}{DN_B + DN_R} \quad (6)$$

Where DN_B and DN_R represent the pixel numbers of Blue and Red channels, respectively.

SI values range from -1.0 to 1.0.

b) B_{BI} [13] $$B_{BI} = \frac{DN_B + DN_G + DB_R}{(2^n - 1) * 3} \quad (7)$$

Where DN_B , DN_R and DN_G represent the pixel numbers of Blue, Red and Green channels, respectively. And n is the bit quantization level number.

c) B_{YUV} [14]: the SI Blue Index using the YUV and YCrCb color spaces is represented by : SI = U / Cb (8)

d) B_T [15] $$B_T = \begin{cases} 1 & se \quad B > \max(R, Tb) \\ 1 & se \quad G : \max(R, Tb) \\ 0 & else \end{cases} \quad (9)$$

Where Tb is a threshold value to ensure that Blue is not too black.

e) B_{BE} [14] $$B_{BE} = 1.4B - G \quad (10)$$

f) B_S [13] $$B_S = \frac{B - R}{B + R'} \quad (11)$$

g) B_I [16] $$B_I = \frac{\sum_{i=216}^{i=256} Bi}{\sum_{j=236}^{j=256} Bj} \quad (12)$$

Where Ri, Gi, Bi are the total number of pixels at each intensity and Rj, Gj, Bj are the value of the intensity.

- *LBP (Local Binary Pattern):* As it is a simple but very efficient description of texture patterns, we chose to use Local Binary Pattern (LBP). The comparison of a center point in its bounded window (usually 3x3) with its neighbors generates a code to replace the value of the center point [17]. This process depends on a threshold according to the equation 13:

$$s \mid x \mid = \left\{ \frac{1, \; Px > P}{0, \quad else} \right\} \quad (13)$$

Where Px corresponds to the center point and P to the neighboring point.

The comparison of a center point with its neighbors is performed as follows:

a. If the center pixel is larger than its neighbor in the circle write '1', otherwise write '0';

b. Thus, we have a code with 8 numbers '0' or '1', ie an 8-bit binary number;

c. Turning this binary number to decimal gives a value between 0 and 255;

d. The descriptor is then composed of these decimal values assigned to each pixel forming the new image.

The representation of the method is shown in figure 4.

104	101	96
97	100	6
102	110	54

1	1	0
0		0
1	1	0

Fig. 4. Process of building an LBP code.

- *EMP (Extended Morphological Profile):* The Extended Morphological Profile by [18] consists in applying opening and closing with increasing structuring element sizes to generate a feature vector according to equation 14:

$$\Omega^{(n)}(I) = \left[\gamma^{(n)}(I), ..., \gamma^{(1)}(I), I, \phi^{(1)}(I), ..., \phi^{(n)}(I) \right] \quad (14)$$

Where $\gamma^{(n)}$, $\phi^{(n)}$ are opening and closing with a disk-shaped structuring element of size n. Then the morphological profiles are obtained in each of the primary components p according to equation 15:

$$\overset{\wedge}{\Omega}_p^{(n)}(I) = \left[\Omega_1^{(n)}(I), \Omega_2^{(n)}(I), ..., \Omega_p^{(n)}(I) \right] \quad (15)$$

In the last step, the morphological profiles are stacked with the spectral response to form the spectral-spatial feature [18].

C. Features Evaluation

To evaluate the efficiency of the features used in this segmentation task, we propose the SVM supervised classifier with the following configuration: Radial Basis Function (RBF) kernel with values of c = 10 and range = 0.0001 in Weka (Waikato Environment for Knowledge Analysis). In the first stage of the research, the best features are obtained by the creation of monolithic classifiers through the 5-fold cross-validation technique. Choosing this evaluation method avoids overlapping test sets [19]. A classifier for each feature vector is thus generated. After individual evaluation, the best features (using the F-measure metric) are combined in the same vector.

The second step consists in combining the output of the classifiers described in the first step. The best whiteness features are combined through the majority vote, that is, the possible combinations between the classifiers evaluated by constructing ensembles of classifiers are considered. To fully use the information obtained from a group of classifiers, the output of each classifier is combined with the others, allowing a decision, the one with the most votes is the winner [20]. This step is employed in two approaches for later comparison. In the first approach, for each base, all images are mixed and separated by 60% for training, generating SVM classifiers for the best individual features and tested with 40% of the images. In the second approach, the same technique is employed, but for each category separately (City, Sea/Harbor, Nature/Mountain, Highway/Road). All training images are divided into two vertical slices. For each slice the sum of the sky/ground pixels is divided by the amount of samples. The result is the pixel range to be selected to generate the training file. For instance, if the number of samples is 400 and the total sum of pixels in the sky is 12000, one pixel will be selected every 12000/400 = 30 pixels for the training file.

To assess each whiteness index in our proposal, we have used the segmentation metrics true positive and negative rates T^+, T^-, false positive and negative rates F^+, F^-, F-Measure *FM* [21] [22]. FM returns 1 for perfect segmentation. The formulation is described in equation 16.

$$FM = \frac{2 * P * R}{P + R} \tag{16}$$

Where $P = \frac{T^+}{T^+ + F^+}$ e $R = \frac{T^+}{T^+ + F^-}$

D. Results and Discussion

This section presents the results of experiments with monolithic classifiers and multiple classifiers.

- *Monolithic Classifier Experiments*

The experiments described below represent the creation of a classifier for each feature vector and the combination of the features in the same vector (grouped features) through the cross validation technique.

Table I depicts the monolithic classifiers created for each feature vector considering the best results.

TABLE I. BEST RESULTS FOR EACH FEATURE VECTOR

Features		F-measure	
		Base Variation	***Base Web***
Whiteness indexes	W_A	89,00%	80,75%
	W_B	92,00%	82,00%
	W_{HL}	92,50%	77,50%
	W_S	92,80%	89,10%
	W_T	90,00%	82,25%
Blueness indexes	B_{BI}	43,00%	39,75%
	B_{BE}	91,25%	82,50%
	B_I	38,50%	34,75%
	B_{SI}	45,50%	43,50%
	B_S	78,50%	62,50%
	B_T	38,50%	34,75%
	B_{YUV}	74,00%	67,75%
LBP		92,20%	88,50%
Extended Morphological Profile		77,10%	75,15%

Figure 5 depicts two images in which the best individual feature was applied.

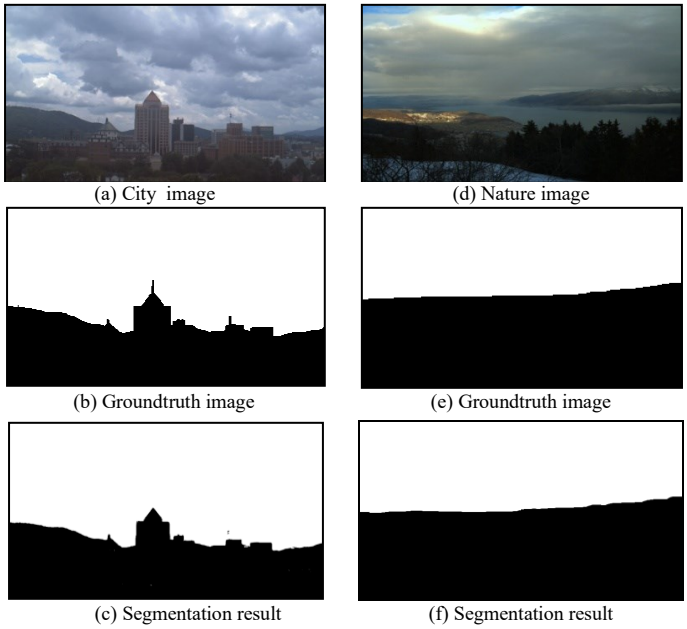

(a) City image (d) Nature image

(b) Groundtruth image (e) Groundtruth image

(c) Segmentation result (f) Segmentation result

Fig. 5. (a) and (c): original images - (b) and (d): groundtruth images - (c) and (f): Segmentation results.

As explained before, some features (using the F-measure metric) are combined in the same vector.

Table II depicts the best whiteness and blue feature combination rates. We can see that the hit rates increase in relation to using only the best whiteness index.

TABLE II. COMBINATION OF WHITENESS AND BLUENESS FEATURES

Image base	W_S + B_{BE}	$W_A + W_B + W_{HL} + W_S + W_T + B_{BE}$
Variation Base	92,10%	89,30%
Web Base	85,90%	80,70%

We can observe that the combination of the whiteness and blue indices did not exceed the W_S, which is the best index found for both databases.

Results with LBP alone were lower than the W_S index. However, as depicted in Table III, the combination of LBP with the best blue index and the five best white indexes (LBP+ $W_A + W_B + W_{HL} + W_S + W_T + B_{BE}$) brought a better F-measure rate in the case of the web database (with 89.40%.). However, this same combination generated F-measure rates below (87%) the results obtained by means of W_S index (91.93%) for the Variation Base.

TABLE III. COMBINATION OF WHITENESS AND BLUENESS FEATURES WITH LBP

Base	LBP + W_S	LBP + W_S + B_{BE}	LBP+ W_A + W_B + W_{HL} + W_S + W_T	LBP+ W_A + W_B + W_{HL} + W_S + W_T + B_{BE}
Variation Base	92,60%	91,93%	91,10%	87,00%
Web Base	88,90%	85,70%	86,80%	89,40%

Similarly, the Extended Morphological Profile was combined with the whiteness and blue indices. As depicted in table IV, the combination the combination (EMP + $W_A + W_B + W_{HL} + W_S + W_T + B_{BE}$), applied to Variation Base, was more interesting since it provides a better result (90.50%). While for the Web Base, the results were below expectations (84.60%). Again, the W_S whiteness index remains the best one.

TABLE IV. COMBINATION OF WHITENESS AND BLUENESS FEATURES WITH EXTENDED MORPHOLOGICAL PROFILE

Base	EMP + $W_A + W_B + W_{HL} + W_S + W_T$	EMP + $W_A + W_B + W_{HL} + W_S + W_T + B_{BE}$
Variation Base	88,78%	90,50%
Web Base	84,60%	83,60%

- *Multiple Classifier Experiments*

In this section, we introduce the idea of creating classifiers for the best features. The first approach consists in mixing images from the various categories and train the best features with 60% of the base and test with the remaining 40%.

While in the second approach, the same protocol is used, this time dividing the images into the four categories: City, Highway/Road, Sea/Harbor, and Nature/Mountain.

First approach - Analysis of results with combination of classifiers for each image base

In this approach, the combination of classifiers considers two classes at a time among the total and, in the end, the result is defined by the majority vote. For each base, the images were mixed and then separated into 60% of the training images, generating an SVM classifier for each of the five best whiteness features. The training images were divided into two slices with 400 pixels of sample. Following, each generated classifier was tested with a set of 40% of the images. From the results we obtained the majority vote or majority vote. Tables V and VI show the experiments performed for the Variation Base and Web Base, respectively.

TABLE V. COMBINATION OF CLASSIFIERS FOR THE VARIATION BASE

Whiteness Indexes	F-measure
W_A	88,30%
W_B	91,50%
W_{HL}	91,90%
W_S	92,80%
W_T	89,60%
Majority Vote	91,11%

TABLE VI. COMBINATION OF CLASSIFIERS FOR THE WEB BASE

Whiteness Indexes	F-measure
W_A	85,40%
W_B	87,40%
W_{HL}	82,60%
W_S	89,10%
W_T	86,60%
Majority Vote	78,16%

In the two databases, the result with the majority vote shows that the W_S whiteness index remains the best. In the case of Variation Base, the results were very close while in the case of Web Base, the majority vote was much lower.

Second approach - Analysis of results with pre-classification of images into categories

As explained earlier, in the second approach, the same protocol is used, this time dividing the images into the four categories previously described. Tables VII to X depicts the results using the Variation Base and Web Base for City, Highway/Road, Sea/Harbor, and Nature/Mountain categories, respectively.

TABLE VII. COMBINATION OF CLASSIFIERS FOR THE CITY CATEGORY

Whiteness Indexes	Variation Base	Web Base
W_A	95,40%	85,40%
W_B	96,90%	89,50%
W_{HL}	96,60%	86,00%
W_S	97,10%	91,31%
W_T	95,90%	86,31%
Majority Vote	96,42%	87,94%

TABLE VIII. COMBINATION OF CLASSIFIERS FOR THE SEA / HARBOR CATEGORY

Whiteness Indexes	Variation Base	Web Base
W_A	89,50%	81,80%
W_B	92,00%	80,11%
W_{HL}	95,00%	77,40%
W_S	93,20%	82,80%
W_T	90,20%	83,70%
Majority Vote	91,82%	82,24%

TABLE IX. COMBINATION OF CLASSIFIERS FOR THE NATURE / MOUNTAIN CATEGORY

Whiteness Indexes	Variation Base	Web Base
W_A	83,80%	91,20%
W_B	87,40%	91,80%
W_{HL}	92,00%	80,00%
W_S	89,40%	92,00%
W_T	85,80%	90,40%
Majority Vote	87,98%	88,60%

TABLE X. COMBINATION OF CLASSIFIERS FOR THE HIGHWAY / ROAD CATEGORY

Whiteness Indexes	Variation Base	Web Base
W_A	88,50%	85,30%
W_B	90,10%	84,80%
W_{HL}	90,20%	87,50%
W_S	91,60%	89,70%
W_T	88,30%	87,00%
Majority Vote	90,04%	86,43%

In this approach, we can see that the W_S whiteness index has lost its supremacy. This whiteness index is the best in the case of Nature / Mountain for the Web Base.

However, while the best results in the City and Highway/Road categories remain with the W_S whiteness index for both databases, in the case of the Sea/Harbor and Nature/Mountain categories, other whiteness indexes are more interesting.

The W_{HL} whiteness index is more efficient for the Sea/Harbor and Nature/Mountain categories, considering the Base Variations.

For the Web Base, the best results are obtained using the W_T whiteness index for the category Sea/Harbor and W_S for the category nature / mountain.

Figures 6, 7, 8 and 9 depict some results.

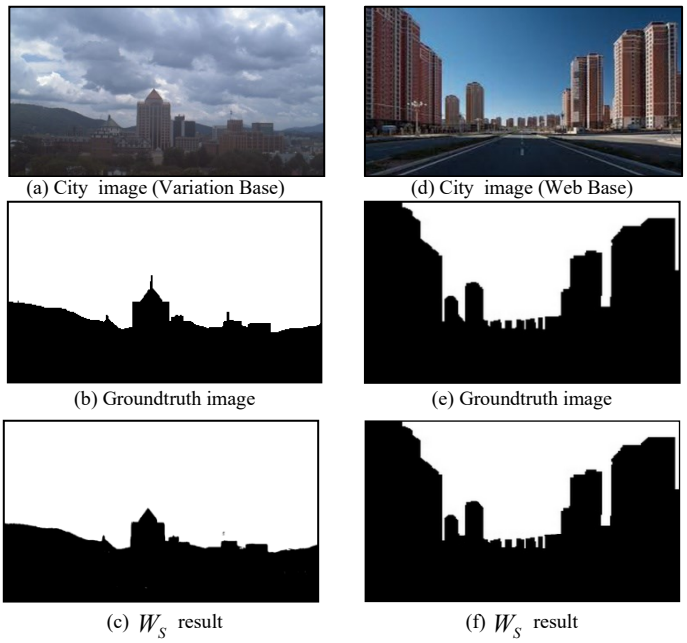

(a) City image (Variation Base) (d) City image (Web Base)

(b) Groundtruth image (e) Groundtruth image

(c) W_S result (f) W_S result

Fig. 6. (a) and (c): original images - (b) and (d): groundtruth images - (c) and (f): Segmentation results with the best index.

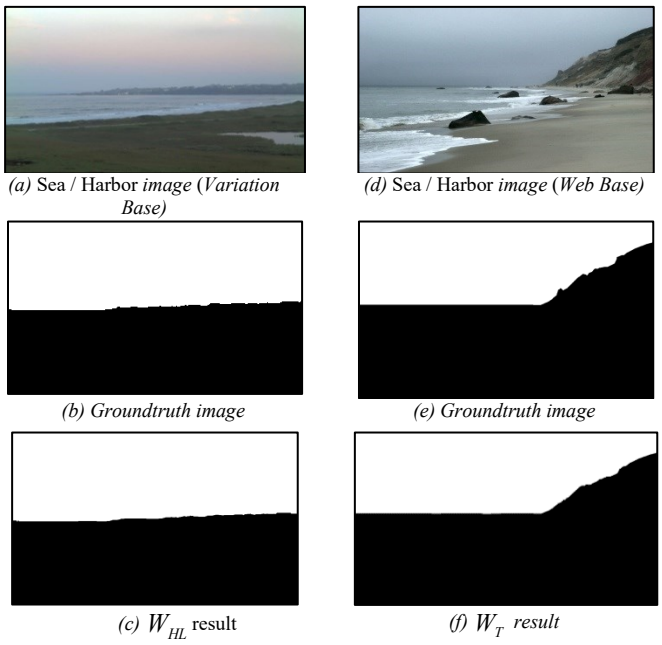

(a) Sea / Harbor *image* (*Variation Base)* *(d)* Sea / Harbor *image* (*Web Base)*

(b) Groundtruth image *(e) Groundtruth image*

(c) W_{HL} result *(f)* W_T *result*

Fig. 7. (a) and (c): original images - (b) and (d): groundtruth images - (c) and (f): Segmentation results with the best index.

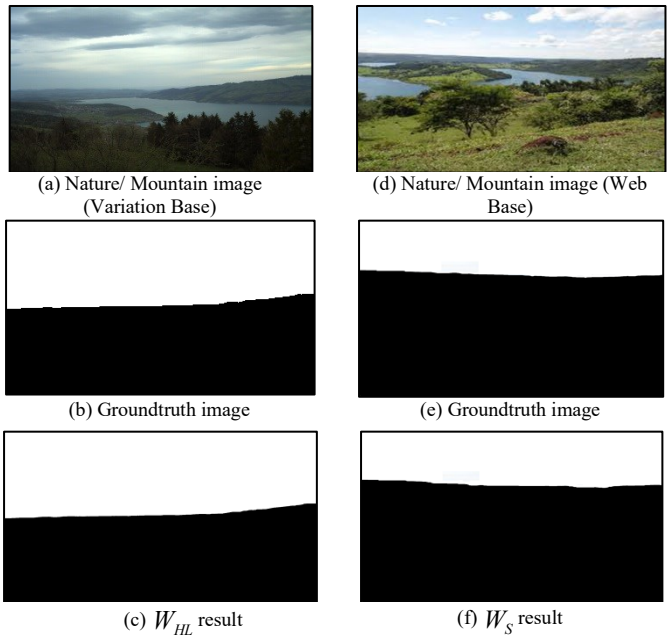

(a) Nature/ Mountain image (Variation Base)

(d) Nature/ Mountain image (Web Base)

(b) Groundtruth image

(e) Groundtruth image

(c) W_{HL} result

(f) W_S result

Fig. 8. (a) and (c): original images - (b) and (d): groundtruth images - (c) and (f): Segmentation results with the best index.

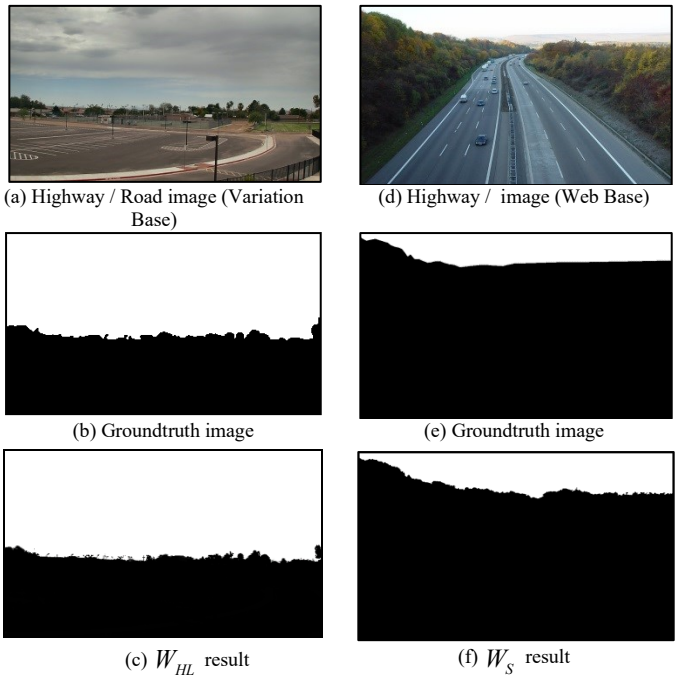

(a) Highway / Road image (Variation Base)

(d) Highway / image (Web Base)

(b) Groundtruth image

(e) Groundtruth image

(c) W_{HL} result

(f) W_S result

Fig. 9. (a) and (c): original images - (b) and (d): groundtruth images - (c) and (f): Segmentation results with the best index.

III. Conclusion

Due to variations in brightness, the presence of different contents such as cities, forests, sea ice, mountains and obstacles such as buildings, trees, antennas, defining an automatic approach to separate sky and ground in digital images represents a difficult task.

We have proposed a two stage sky/ground segmentation approach: in the first one, generally adopted in the literature, the best features are selected by monolithic classifiers using the cross-validation technique. In second one, we introduce the idea of creating classifiers for the best features and segmenting sky and ground with combination (fusion) of classifiers, with the option of dividing the databases or not.

Two databases of 1200 images each composed of City, Highway/Road, Sea/Harbor, Nature/Mountain have been created to run the experiments.

The second approach, still little used in the literature, aimed to assess the impact of the presence of cities, forests, sea ice, mountains on the segmentation rates as well as to compute the importance of categorizing the images according to different contents.

In all numerical evaluations, the segmentation metric F-measure was used.

The results of the experiments proved that in the case of the best features selected by monolithic classifiers using the cross-validation technique, no combination was more successful than the W_S whiteness index, regardless of the content of the images.

When using classifiers for the best resources and combination (fusion) of classifiers, with the option of dividing the databases or not, the experimental results proved that higher sky/ground segmentation rates can be obtained, conditioned to the content of each image.

The final conclusion of this research was that we observed the impact that different contexts of terrain, climate and have on the performance of the methods.

As a future work, we intend to associate deep learning techniques to the features mentioned in this work with images without pre-processing or pre-processed.

References

[1] Lie, W.-N., Lin, T.C.-I., Lin, T.-C., Hung, K.-S., “A robust dynamic programming algorithm to extract skyline in images for navigation”, Pattern Recognition Letters 26, pp. 221–230, 2005.

[2] Bao, G. Q.; Xiong, S. S.; Zhou Z. Y., “Vision-based horizon extraction for micro air vehicle flight control”, IEEE Transactions on Instrumentation and Measurement, vol. 54, no. 3, pp. 1067-1072, 2005.

[3] Stephen Williams and Ayanna M. Howard, ”Horizon Line Estimation In Glacial Environments Using Multiple Visual Cues“, IEEE International Conference on Robotics and Automation, ICRA 2011, Shanghai, China, pp. 5887—5892, May 2011.

[4] Croon, G.C.H.E., De Wagter, C., Remes, B.D.W., Ruijsink, R., “Sky Segmentation Approach to Obstacle Avoidance”, IEEE Aerospace Conference 2011, pp. 1 - 31, 2011.

[5] Lipschutz Ilan, Gershikov Evgeny, Milgrom Benjamin, “New Methods for Horizon Line Detection in Infrared and Visible Sea Images”, International Journal Of Computational Engineering Research (ijceronline.com) Vol. 3 Issue. 3. pp. 226 -233, 2013.

[6] Verbickas, Rytis; Whitehead, Anthony, “Sky and Ground Detection Using Convolutional Neural Networks”, Proceedings of the International Conference on Machine Vision and Machine Learning Prague, Czech Republic, August 14-15, 2014.

[7] De Mattos, Flávia; Beuren, Arlete Teresinha; de Souza, Bruno Miguel Nogueira; De Souza Britto, Alceu; Facon, Jacques, “Supervised Approach to Sky and Ground Classification Using Whiteness-Based Features” In: Lecture Notes in Computer Science.2 ed. : Springer International Publishing, 2018, p. 248-258.

[8] Andrew Joiner, Ian Hopkinson, Yan Deng, Stephen Westland, “A review of tooth colour and whiteness”, Journal of Dentistry Volume 36, pp. s2-s7, 2008.

[9] Lin Juan, ”Factors Affecting the Perception and Measurement of Optically Brightened White Textiles”, PhD Thesis, Graduate Faculty of North Carolina State University Raleigh, North Carolina, p. 366, 2013.

[10] X-rite, “Color iQC and Color iMatch Color Calculations Guide”, Version 8.0, p. 31, July 2012.

[11] Claudio Puebla, “Whiteness Assessment: A Primer”, Axiphos GmbH. Germany, p. 64, 2006.

[12] Watanabe, S.; Vincent, W. F.; Reuter, J.; Hook, S. J.; Schladow, S. G., “A quantitative blueness index for oligotrophic waters: Application to Lake Tahoe”, California–Nevada. Limnol. Oceanogr. Methods, 14: 100–109. doi:10.1002/lom3.10074. 2016.

[13] Yamashita, M.; Yoshimura, M., “Ground-based cloud observation for satellite-based cloud discrimination and its validation”, International Archives of the Photogrammetry, Remote Sensing and Spatial Information Sciences, Volume XXXIX-B8, pp. 137- 140, 2012.

[14] Castro, Ana I. de. Ehsani, Reza; Ploetz, Randy C.; Crane, Jonathan H.; Buchanon, Sherrie., “Detection of Laurel Wilt Disease in Avocado Using Low Altitude Aerial Imaging”. PLoS ONE 10(4), pp.1-13, 2015.

[15] Loui, Alexander C.; Savakis, Andreas E., “Automatic Image Event Segmentation and Quality Screening for Albuming Applications”, IEEE International Conference on Multimedia and Expo, New York City, New York, pp 1-4, July 2000.

[16] Mishra, Pavan Kumar; Maurya, Sanjay Kumar; SINGH, Ravindra Kumar, MISRA, Arun Kumar., “A semi automatic plant identification based on digital leaf and flower Images”, IEEE-International Conference On Advances In Engineering, Science And Management (ICAESM -2012), pp 68-73, 2012.

[17] Ojala, T.; Pietikainen, M.; Maenpaa, T., “Multiresolution gray-scale and rotation invariant texture classification with local binary patterns”, Pattern Analysis and Machine Intelligence, IEEE Transactions on, [S.l.], v.24, n.7, p.971–987, 2002.

[18] Liang, Jie; Zhou, Jun; Gao, Yongsheng., “Tensor Morphological Profile for Hyperspectral Image Classification”, 2016 IEEE International Conference on Image Processing (ICIP), 2016.

[19] Yu-Quan, Zhu; Geng, Chen; Hai-Ping, Yu., “Dynamic weighting ensemble classifiers based on cross-validation”, Neural Computing & Applications, v. 20, n. 3, pp. 309-317, 2011.

[20] Breiman, Leo, “Bagging Predictors. Machine Learning”, Vol. 24, p. 123-140, 1996.

[21] Bimbo, A. D., “Visual information retrieval”, Morgan Kaufmann, 1999.

[22] Gatos, B.; Nitirogiannis, K.; Pratikakis, I., “Document image binarization contest”, ICDAR - International Conference on Document Analysis and Recognition, p.1375 - 1382, 2009.

[23] Mihail, Radu P.; Workman, Scott; Bessinger, Zach, “Sky segmentation in the wild: An empirical study”. *Applications of Computer Vision (WACV), 2016 IEEE Winter Conference on*. IEEE, 2016.